Full-wave inversion (FWI) to a 2D-ocean-bottom node (OBN) dataset after offset-continuation-trajectory (OCT) data regularization

Alexandre Camargo (CEPETRO/UNICAMP), José Ribeiro (CEPETRO/UNICAMP), Tiago A. Coimbra (CEPETRO/UNICAMP), Gustavo B. Ignácio (CEPETRO/UNICAMP), and Martin Tygel (CCES/CEPID and CEPETRO/UNICAMP)

This paper was prepared for presentation at the 16th International Congress of the Brazilian Geophysical Society, held in Rio de Janeiro, Brazil, August 19-22, 2019.

Abstract

The estimation of geophysical attributes for a better understanding of subsurface geological structures is essential in many stages of seismic exploration and production. As a powerful seismic inversion tool, the full waveform inversion (FWI) has been widely used to estimate many of such attributes (e.g., seismic velocities) with high resolution. In many cases, however, real acquisitions are unable to provide the quantity and density of traces required for optimal inversion results. As a consequence, schemes to produce (simulate) new traces by interpolation/extrapolation of neighboring available traces, play a crucial role. In this paper, we use the offset-continuation-trajectory (OCT) stacking method to generate new (non-recorded) traces and include them in an ocean-bottom node (OBN) acquisition. We next test the FWI inversion on the enhanced dataset and analyze the results. As proof-of-concept, our approach is applied to the synthetic dataset obtained for an OBN acquisition carried out on the 2D Marmousi model for which several additional traces, simulated by the OCT procedure, have been included. In spite of the recognized complexities of the Marmousi model, we have obtained very encouraging results.

Introduction

Full-wave field inversion (FWI) is a method to obtain high-resolution subsurface velocity models. The procedure is based on the complete wave field modeling to obtain synthetic seismograms. The difference between the amplitudes of observed (real) and synthetic events of interest serves to perform an inversion process of updating the velocity model.

As it is the general case for inversion methods, FWI is expected to provide better results whenever a dense distribution of shots and receivers is available. Quite often, however, acquisition configurations are unable to provide such required trace conditions. As such, schemes, interpolation/extrapolation methods that are able to simulate new (unregistered traces) from neighboring (registered) traces are always in demand. In particular, such schemes have the potential of enabling cost-reduced acquisitions as fewer traces need to be recorded. As described in (Coimbra et al., 2012, 2016) and based on the common-reflection-surface (CRS) parameters, the offset-continuation-trajectory (OCT) is able to simulate from a given common-offset section determined for a given half-offset, the corresponding *continued* common-offset section that corresponds to a new, user selected, different half-offset. In this way, the OCT method can be used as a trace-simulation tool so as to provide trace-enhanced datasets better fit for FWI.

A question that naturally arises is whether a dataset enhanced with simulated traces is still able for FWI application. That depends, not only to the accuracy of the trace simulation, but also on the robustness of the FWI procedure. In this paper, we address this problem, we consider a synthetic dataset of an ocean-bottom-node (OBN) acquisition geometry (see, e.g., Gaiser, 2016), computed with the 2D Marmousi velocity model (Versteeg, 1994). We compare the FWI results obtained with the original, full-trace datasets with corresponding ones obtained upon the replacement of some of the original traces with simulated ones computed with OCT. For our numerical experiments, the answer of the previous question is affirmative. Namely, the FWI results in both cases are very similar. This encourages, as further natural steps, the consideration of the procedure on real datasets, so as to make it practically feasible.

Figure 1 illustrates a typical OBN geometry.

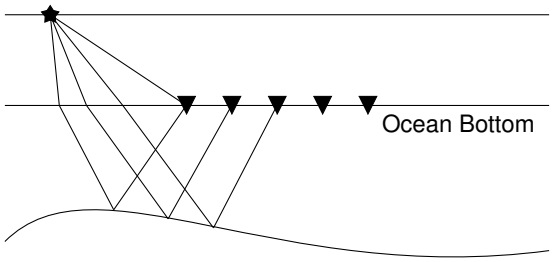

Figure 1: Typical sketch geometric of an OBN acquisition.

Formulation

We briefly describe the algorithms of FWI and OCT algorithms used in this work. As our main focus is to actually test the proposed combination of FWI and OCT to a specific dataset, we refrain to provide the technical exposition of these algorithms, referring the interested reader to adequate publications available in the literature.

FWI

For a given acquisition configuration, FWI is carried out as an iterative, which consists of solving a forward and an inverse problems. An initial model for the attributes desired to be inverted is supposed to be provided. In our case, the single attribute of acoustic velocity is considered. With the help of that initial model, the forward problem consists of computing all the shot records available in original dataset. That computation is carried out by solving the acoustic wave equation under the use of a finite-differences modeling (FDM) scheme. For inverse problem, the obtained shot records are compared with their corresponding observed ones, giving rise to a misfit values that are be iteratively minimized in least-squares sense. Thus, those misfits are used to produce a new, updated velocity model. The process is iterated until a given stop criterion is reached. As indicated above, we are here only concerned with actual applications only, so that a technical description of the algorithms of FDM and FWI theory is out of the scope of this paper. For the interested readers, we recommend the excellent tutorial Virieux and Operto (2009), as well as the thesis Camargo (2019) for more specific details concerning the algorithms used in this work.

OCT

The OCT trace-simulation procedure is based on the offset-continuation operation (OCO) described in (Coimbra et al., 2012, 2016). This operation transforms traces on a registered common-offset section defined of a given half-offset, into corresponding (unregistered) common-offset traces of a different, *continued* half-offset. In this way, non-existent traces that belong to a common-offset section can be simulated by registered traces that belong to a common-offset section of a neighboring half-offset. As previously, we refrain of providing the mathematical exposition of the OCT algorithm, referring the reader to the above publications.

As a final remark, we mention that the development and coding of all algorithmic used in this paper have been carried out in house at the High-Performance Geophysics (HPG) Laboratory at the Center for Petroleum studies (CEPETRO) at the University of Campinas (UNICAMP).

Numerical Experiments

The following numerical experiments are analysed using the OCT method in the datasets. After that, we apply the FWI method to analyze the effects that occur in the velocity estimation using the regularized observed data.

As depicted in Figure 1, we consider the idealized situation of an ocean-bottom-node (OBN) seismic acquisition performed on the Marmousi velocity model (Versteeg, 1994) subsurface illustrated in Figure 2. Under such conditions, an observed dataset, called the Reference dataset is simulated. As described by the second column of Table 1, the Reference dataset consists of shot records that correspond to 401 surface point sources and 61 receivers at a planar sea bottom surface located at 500 m depth. The shot records are simulated as the solutions of the acoustic wave equation, these being obtained by the finite-difference method (FDM) for a centered scheme of second order in time and eighth order in space (Strikwerda, 1947). The point source is given by a Ricker wavelet with peak frequency of 20 Hz. The FDM parameters, which satisfy the numerical criteria of stability and dispersion, are $\Delta x = \Delta z = 10$ m, $\Delta t = 1$ ms for a maximum recording time $T = 2$ s. Besides the Reference dataset, we also consider

Table 1: Dataset acquisition parameters for the Reference, Case 1 and Case 2 datasets

	Experiments		
Parameters	Reference	Case 1	Case 2
Number of shots	401	401	41
Number of receivers	61	21	61
Shot separation (m)	20	20	200
Receiver separation (m)	100	300	100
Maximum offset (km)	7	7	7

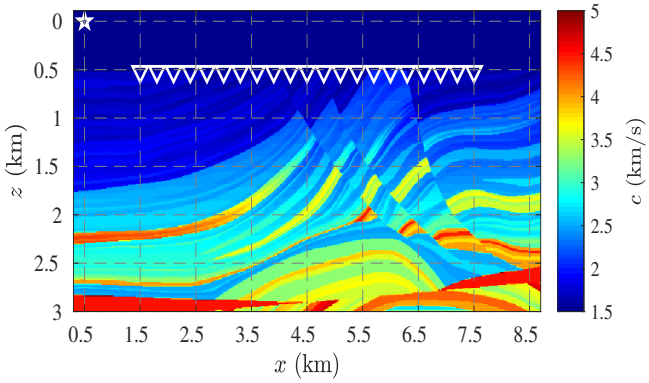

Figure 2: Marmousi depth-velocity model. $\triangledown$ represent receiver positions at ocean bottom and $\star$ represents a shot at sea surface.

two additional datasets, designated by Case 1 and Case 2 datasets, with acquisition parameters provided by the third and fourth colums of Table 1, respectively. These datasets will be used to test the FWI for regularized versions of the Case 1 and Case 2 datasets obtained by OCT trace-simulated inclusions. The difference between Case 1 and Case 2 is the number and spacing of shots and receivers. Case 1 has better illumination than Case 2, however with a less dense distribution of receivers. Figures 3 (a), 3 (b) and 3 (c) show a central shot record with shot coordinates $\boldsymbol{x}_s = (4.5 \text{ km}, 0)$, within the Reference, Case 1 and Case 2 datasets, respectively. As previously indicated, the Reference dataset will be used for comparison with regularized Case 1 and Case 2 datasets regularized (i.e., with inclusion of OCT simulated traces).

Regularization

OCT stacking regularization is applied for seismic traces that, in principle, were not recorded in the original data, but are well approximated by OCT simulation. As described in Coimbra et al. (2012, 2016), the OCT trace simulation makes use of the CRS parameters, midpoint slope and half-offset curvature (or time velocity). Such parameters are directly extracted from the original data, being initialized for the zero-offset (stacked) data and next iteratively updated for increasing half-offsets. Even not going into

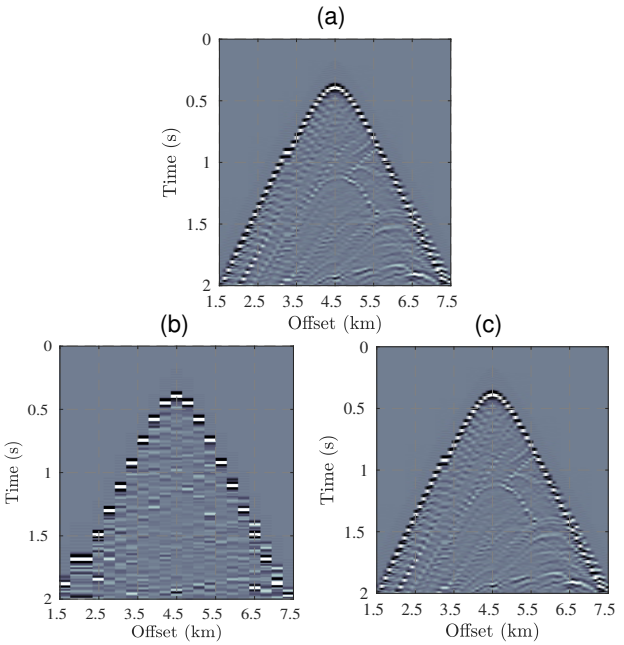

Figure 3: Observed data for shot at position in (4.5 km,0) representing a field acquisition: (a) Reference dataset; (b) Case 1 dataset; (c) Case 2 dataset.

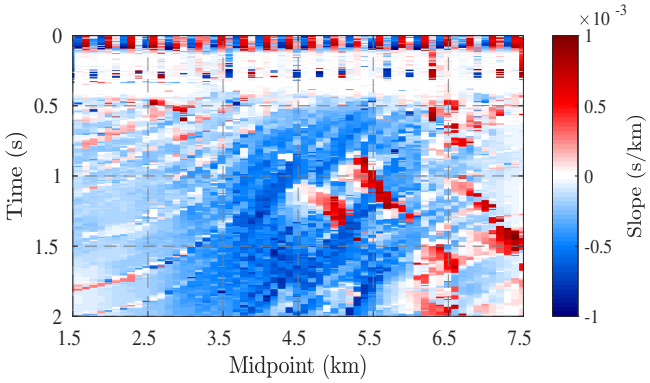

Figure 4: The initial slope OCT parameter in zero-offset gather estimated from Case 2 dataset.

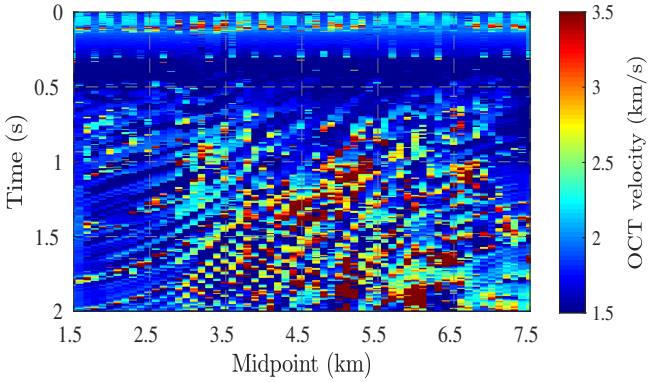

Figure 5: The velocity OCT (or OCO) parameter in zero-offset gather estimated from Case 2 dataset.

details about the CRS parameter-estimation algorithms, we provide, for completeness, using the Case 2 dataset, Figure 4 and Figure 5 in which the initial (zero-offset) midpoint slopes and time velocities are shown. These two parameters used in OCT trajectory are estimated using a given dataset on the reference geometry, i.e., 401 shots and 61 receivers, with maximum offset-aperture of 750 m. However, a more careful analysis would provide more accurate parameters. Besides that, the initial seismic dataset used in OCT procedure has the direct wave events removed and the recording time is longer due to boundary problems, that is, the direct wave event is not obtained by the approximation. However in OBN acquisition this is not relevant, since the receiver are positioned in ocean bottom.

It is to be remarked that the OCT simulation produces regularized, full seismic gathers, including already recorded ones. In these situations, we can replace the OCT-simulated (approximate) traces with the corresponding, originally recorded ones.

Regularized common-shot gathers obtained by OCT trace-simulation without replacement of originally existing traces are shown in Figures 6 (a) and 6 (b) for Case 1 and Case 2 datasets, respectively.

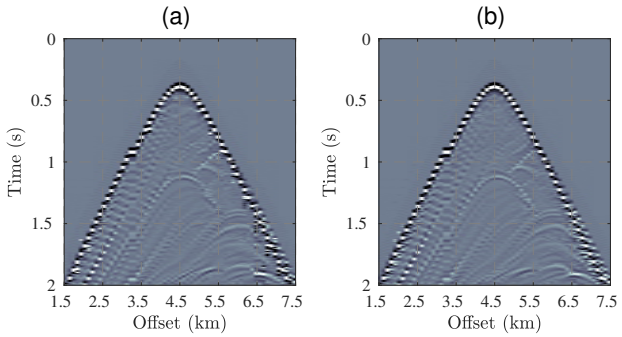

Figure 6: "Observed" data obtained by OCT for shot at position in (4.5 km,0) using: (a) Case 1 dataset; (b) Case 2 dataset.

In the same way, Figures 7 (a) and 7 (b) show zero-offset gather shown computed for the original (non-regularized) Case 1 and Case 2 datasets. These sections are to be compared with the ones of Figures 8 (a) and 8 (b), show the zero-offset sections computed after regularization of the Case 1 and Case 2 datasets, respectively. In addition, Figure 8 (c) show the zero-offset gather computed for the original Reference data. Comparison of the first to sections (which refer to Case 1 and Case 2 datasets) with the third section (which refers to the Reference dataset) indicate that the regularization provided very satisfactory results, with nonphysical artifacts being not present.

Figures 9 (a) and 9 (b) now compares, for a single trace position at 4.3 km, the corresponding traces obtained after regularization of Case 1, Case 2 datasets with the non-regularized, original Reference dataset. Notice that, in Case 1 dataset, there is no receiver at that position, but was generated by regularization. While, in Case 2 dataset all receivers exist and the regularization occurs in the number of shots. Soon, becomes a good reference to analyze the precision for Case 1 dataset, since the central shot position there is in all dataset.

FWI

We now focus on the FWI application method to our given datasets. Our FWI computation uses the quasi-Newton

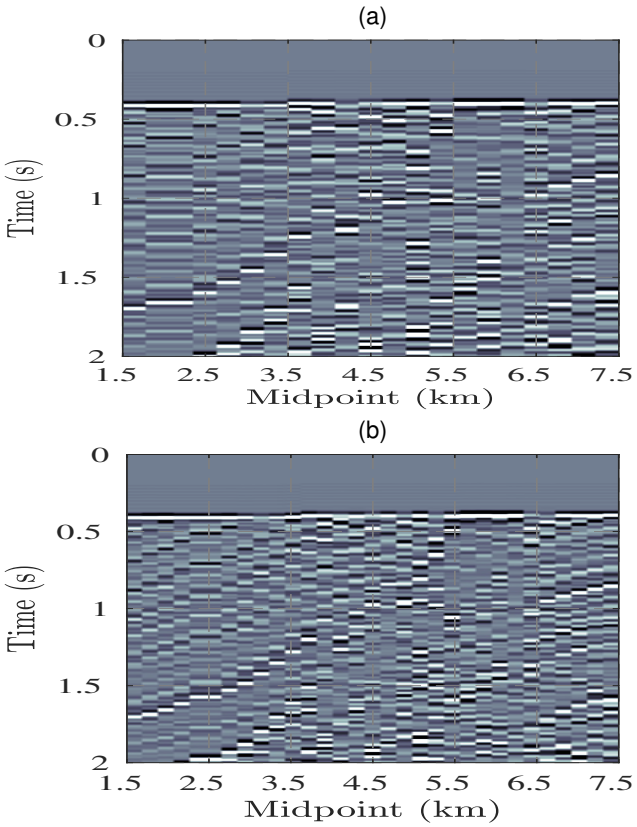

Figure 7: Zero-offset gather for: (a) Case 1 dataset; (b) Case 2 dataset.

optimization method Limited-memory-Broyden-Fletcher-Goldfarb-Shanno (L-BFGS) proposed by Liu and Nocedal (1989), where the step length is determined by Armijo's rule (sufficient decrease) together with the curvature condition, these two jointly conditions are commonly called by strong Wolfe condition (Nocedal and Wright, 1999). The optimality tolerance parameters $\varepsilon = 10^{-05}$ and maximum iteration is 100. We suppose that the sea bottom is planar an at depth z =500 m and the water water velocity is 1.5 km/s. In the inverse process the same numerical scheme of finite-difference is used, but with fourth order approximation in space. All the implementation was done in GPU.

The initial velocity model for our FWI computations in all experiments is illustrated in Figure 10. This model was obtained by applying smoothing filter, i.e., a central moving average applied in eighty-one points for each side to the original Marmousi model.

Figures 11 (a), 11 (b) and 11 (c) show the final velocity model using observed, non-regularized datasets for Case 1, Case 2 and Reference model, respectively. Comparing with Figure 11 (c), Figure 11 (a) (which refers to Case 1) in the region [5.5,8.5]$\times$[0.5,1.5] (in km) shows a smoothing, while Figure 11 (b) (which refers to Case 2), in the same region, in relation to Figure 11 (a) presents a noisier aspect, which is due to the low illumination (i.e., smaller numbers of shots), even with a larger distribution of receivers. However, comparing with true model (Figure 2) around the coordinate (6.5 km, 1.5 km) we have lose resolution and continuity in the three models depicted. Aside from this, the estimated velocities are

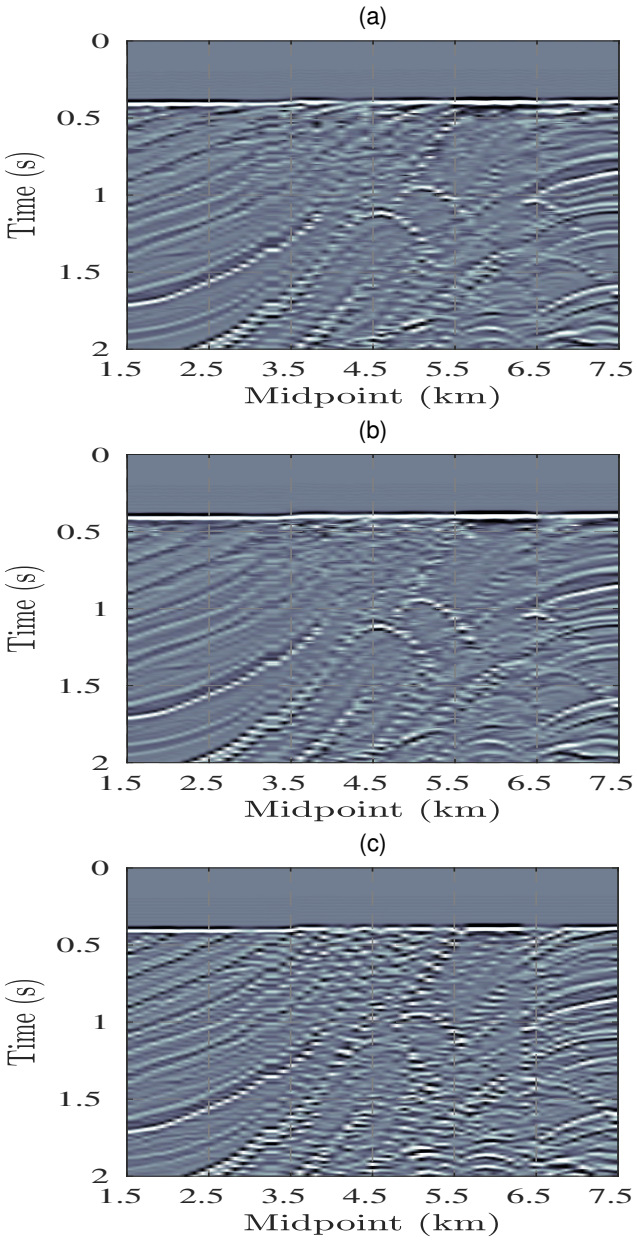

Figure 8: Zero-offset gather for: (a) Regularized Case 1 dataset; (b) Regularized Case 2 dataset; (c) Reference dataset.

below compared to the true ones, but we do not use any regularization/penalization strategies or filters that can help in final solution as multi-scale strategies (Bunks et al., 1995).

Figures 12 (a) and 12 (b) show the estimated model for the Cases 1 and 2 datasets after regularization, respectively. The seismic traces used as observed data were obtained by OCT, that is, we not use the real traces available. In both solutions, the estimated model are with resolutions very close to the reference model (Figure 11 (c)), but the approximation obtained is a little more smooth. Nevertheless, in coordinate (6.5 km, 1.5 km) we have a region with better resolution and continuity than reference solution and in region [2.5,4.5]$\times$[1.5,2] (in km) the approximation also is better compared to that shown in

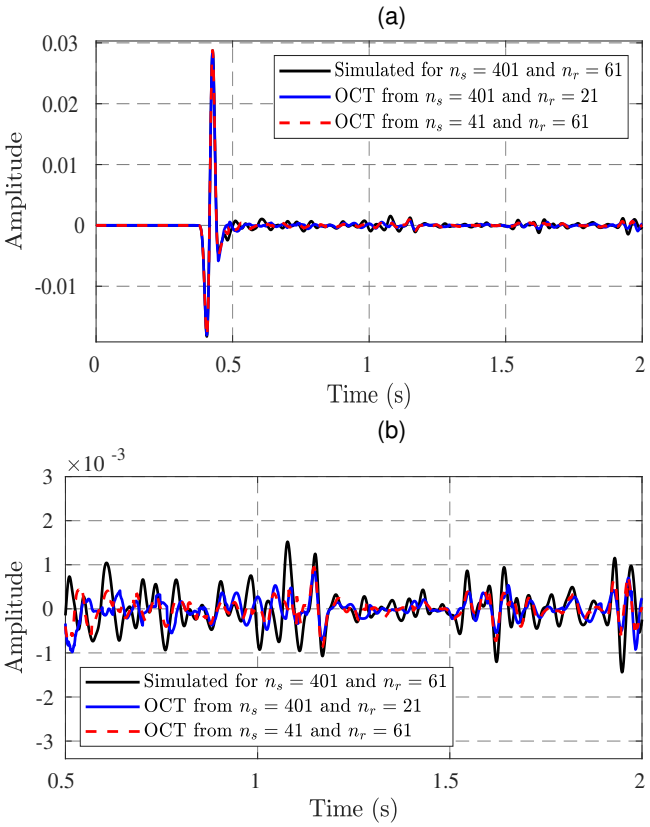

Figure 9: (a) Comparison between OCT traces with reference model at position 4.3 km ; (b) Detail in the reflection events.

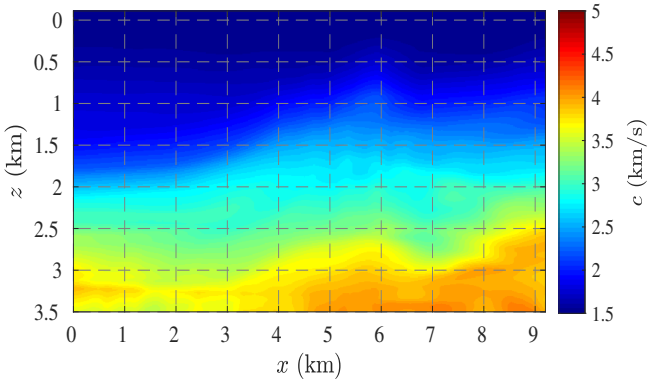

Figure 10: Initial approximation for the velocity model used in FWI method .

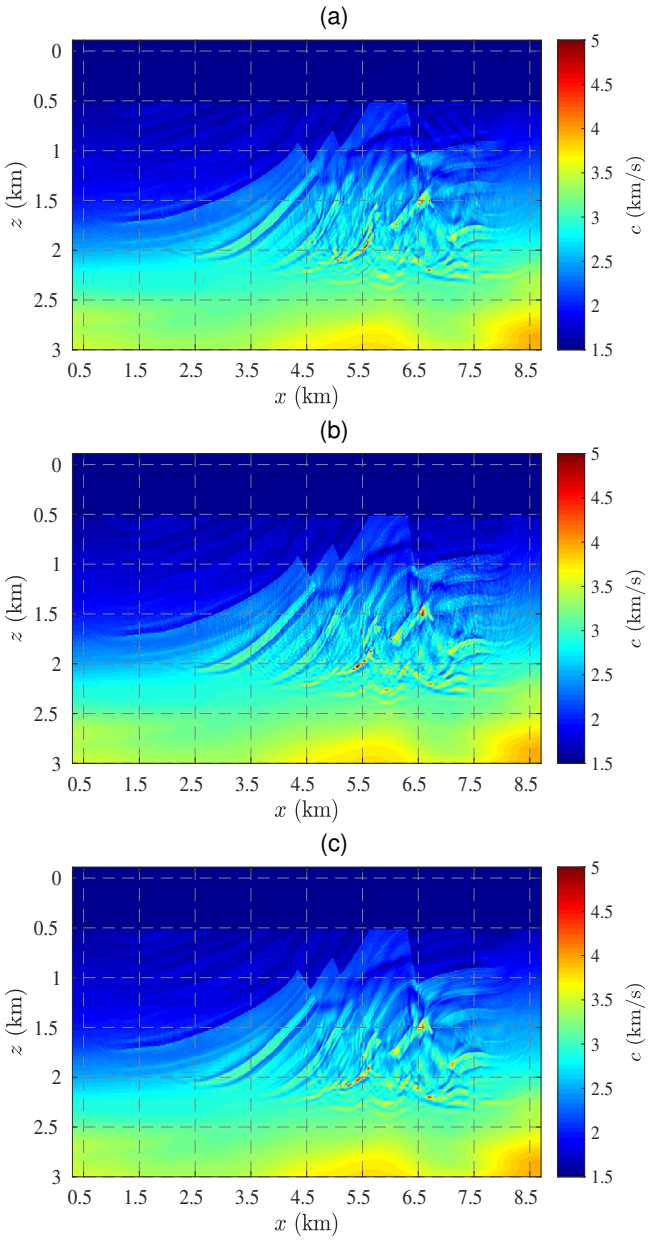

Figure 11: Estimated velocity model at iteration 100 using observed, non-regularized datasets: (a) Case 1; (b) Case 2; (c) Reference model.

Figures 11 (a) and 11 (b). But, in quadrant with center at (4.5 km,1.0 km) we have a loss of resolution.

Figures 13 (a) and 13 (b) show the estimated model by FWI, where the observed data contain the seismic traces are already available in the field plus the traces covered by OCT regularization. Note that the characteristics were practically maintained, however in the region that had loss present a slight better resolution now. Therefore, the FWI solution using the observed data obtained by OCT regularization show to be an alternative to decrease the operating cost of an OBN acquisition, since the solutions obtained show a quality very close to the reference model compared by same criteria in seismic inversion.

Conclusions

In this work, we show an alternative to reduce cost of an OBN acquisition, but it does not restrict only to this type of acquisition. The solution shows very similar to the solution of the reference model, that is, there are any significant losses, but in some regions we have even improved. Based on ours experiments, we believe that solutions can be improved by applying an meticulous analysis on OCT parameters and to adopt multi-scale strategy on FWI method. This technique can improve the illumination of the reflectors which can sometimes be a problem simply because there may be no way to position receivers in certain regions.

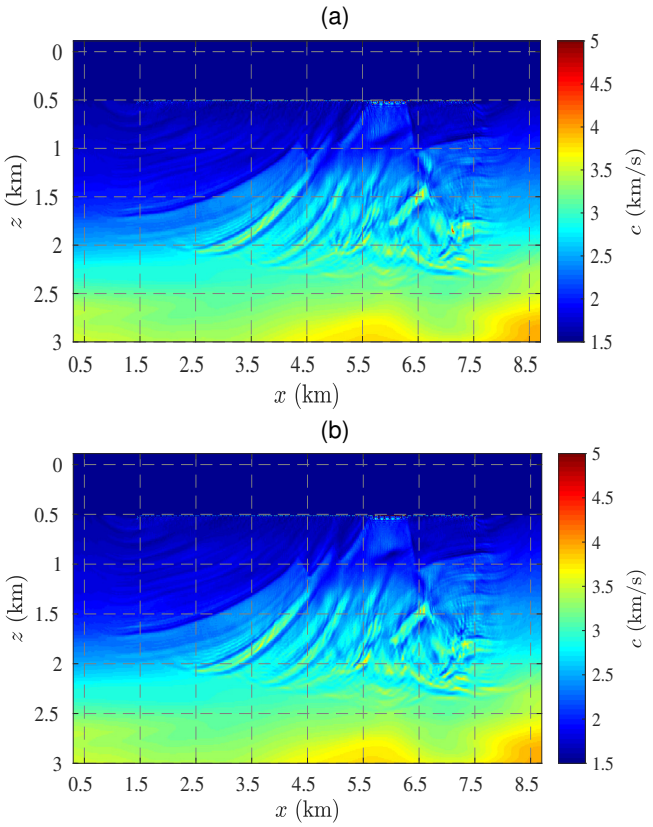

Figure 12: Estimated velocity model at iteration 100 using OCT regularized datasets (a) Case 1; (b) Case 2.

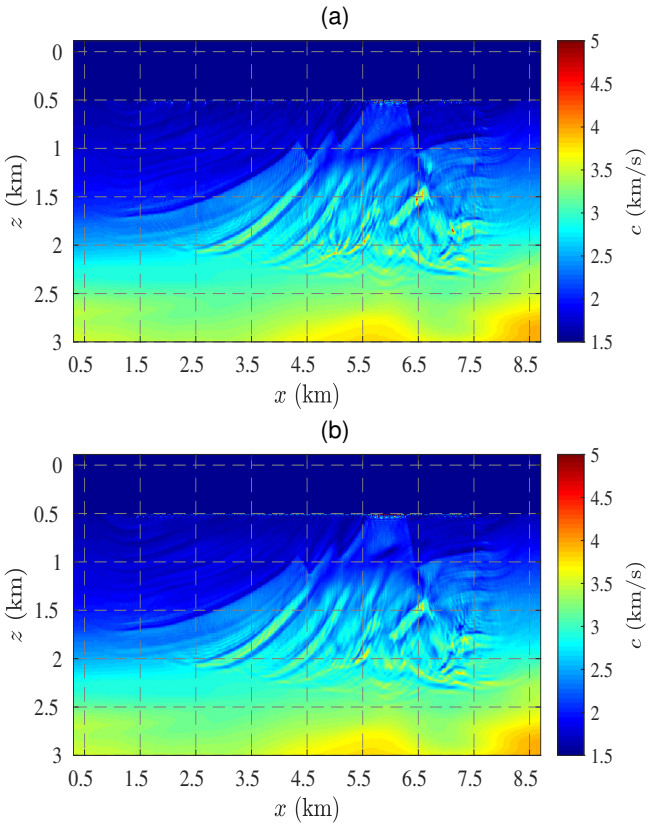

Figure 13: Estimated velocity at iteration 100 using observed data obtained by OCT regularization replacing with real traces: (a) Case 1; (b) Case 2.

Acknowledgments

This work was possible thanks to the support of Petrobras and Fapesp/Cepid #2013/08293-7-Brazil. The authors also thank the High-Performance Geophysics (HPG) team for technical support.

References

Bunks, C., F. M. Saleck, S. Zaleski, and G. Chavent, 1995, Multiscale seismic waveform inversion: Geophysics, **60**, 1457–1473.

Camargo, A. W., 2019, Analysis of the full waveform inversion using the augmented lagrangian method (In Portuguese).

Coimbra, T. A., A. Novais, and J. Schleicher, 2012, Offset-continuation (OCO) ray tracing using OCO trajectories: Studia Geophysica et Geodaetica, **56**, 65–82.

———, 2016, Offset-continuation stacking: Theory and proof of concept: Geophysics, **81**, V387–V401.

Gaiser, J., 2016, 3c seismc and VSP: Converted waves and vector wavefield applications: Society of Exploration Geophysicists. Distinguished Instructor Series.

Liu, D. C., and J. Nocedal, 1989, On the limited memory bfgs method for large scale optimization: Mathematical Programing, **45**, 503–528.

Nocedal, J., and S. W. Wright, 1999, Numerical optimization: Springer.

Strikwerda, J. C., 1947, Finite difference schemes and partial differential equations: Society for Industrial and Applied Mathematics.

Versteeg, R., 1994, The marmousi experience: Velocity model determination os a synthetic complex data set: The Leading Edge, **13**, 927–936.

Virieux, J., and S. Operto, 2009, An overview of full-waveform inversion in exploration geophysics: Geophysics, **74**, 127–152.